Organic & Biomolecular Chemistry

www.rsc.org/obc

Volume 8 | Number 16 | 21 August 2010 | Pages 3581–3808

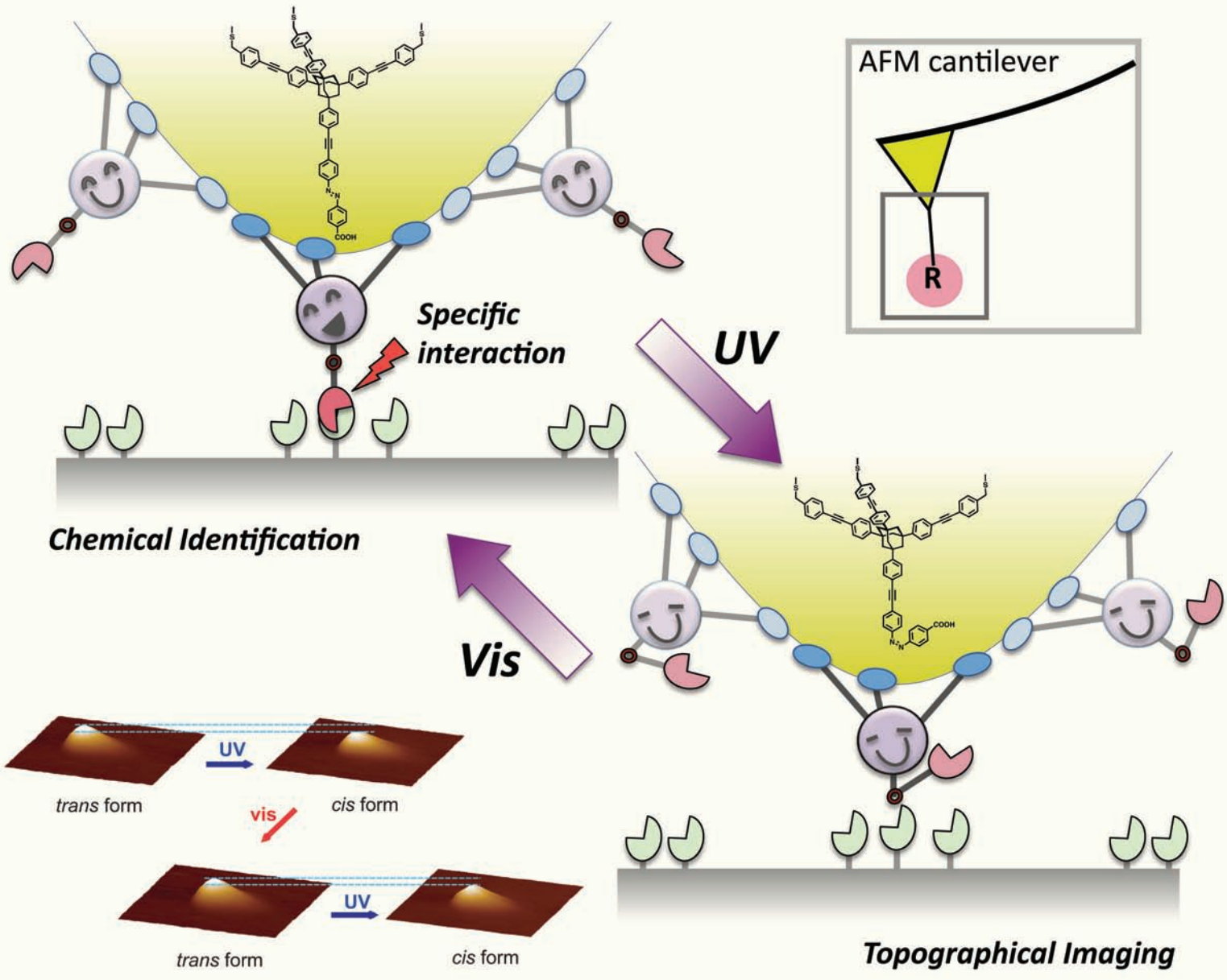

ISSN 1477-0520

RSC Publishing

Photoswitching tripodal single molecular tip for noncontact AFM measurements: synthesis, immobilization, and reversible configurational change on gold surface†

Daiko Takamatsu,[a] Ken-ichi Fukui,*[b,d] Safwan Aroua[c] and Yoko Yamakoshi*[c,d]

Received 11th February 2010, Accepted 24th May 2010
First published as an Advance Article on the web 30th June 2010
DOI: 10.1039/c002657c

Tripodal molecules consisting of a tetrasubstituted adamantane with three phenylacetylene legs and a reversibly photoswitching apex were designed as "single molecular tips" for both chemical and topographical characterization of the substrate surface. By covalent attachment onto gold-coated AFM tips through three S–Au bonds, these rigid tripodal molecules are expected to act as sharp, robust, and stationary molecular tips whose configuration can be reversibly changed upon irradiation with UV or visible light. In this report, the full account of the syntheses of two photoswitching tripodal molecular tips, their immobilization onto Au(111) surfaces, and the detection of photoinduced configurational change on Au(111) surface by SPM measurements are documented.

Introduction

Nanotechnological developments including scanning probe microscopies (SPMs) have enabled nanometer scale analysis of the surface, often with atomic resolution. In particular, atomic force microscopy (AFM)[1] is applicable to the imaging of non-conductive samples including biomolecules. Common materials for AFM tips are silicon, silicon nitride and gold, and usually possess sharp apexes with nm-scale radii, which directly affects the resolution of the AFM image obtained upon scanning a surface. Whereas the topographical information of the surface can be obtained by AFM imaging, it is generally impossible to detect the chemical or functional characteristics of the surface using normal AFM tips.

The introduction of specific functionality onto the AFM tip surface by the attachment of organic molecules has enabled the detection and study of the chemical properties of the substrate surface using chemical force microscopy (CFM). In initial CFM studies, including those by Lieber and co-workers,[2] a simple self-assembled monolayer (SAM) system with alkanethiol–gold chemistry was used as a convenient method for AFM tip functionalization. In the following decade of CFM studies, it has become important to have an appropriate design of the organic molecules to serve as a "single molecular tip". Critical properties in the design of such molecules include a suitable orientation and stability of the molecules when they are attached onto the AFM tip surface. Several designs of organic molecular tips for AFM functionalization have been provided by synthetic chemists, including single wall-nanotube (SW-NT)[3] and tripodal molecules[4–9] as basic skeletons for the "single molecular tip".[10]

In this study, we designed a "tripodal molecular tip" (Fig. 1) with a rigid adamantane–phenylacetylene scaffold[6,7] and a photoswitching azobenzene[11] for both (1) the chemical characterization and (2) the topographical imaging of the surface. The tripodal scaffold was expected to generate a suitable orientation of the molecule with three covalent S–Au bonds to support tightly the molecule through straight and rigid phenylethynyl legs. In contrast to the general SAM systems with alkanethiol derivatives for AFM tip modifications where molecules are immobilized in an assembled form also *via* horizontal hydrophobic interactions, the tripodal molecules are expected to attach on the gold surface in an isolated form. In addition, the phenylacetylene apex of the molecule will be perpendicular to the gold surface horizon and serve as an extremely sharp tip. The further introduction of a photosensitive azobenzene in the apex enables light-controlled

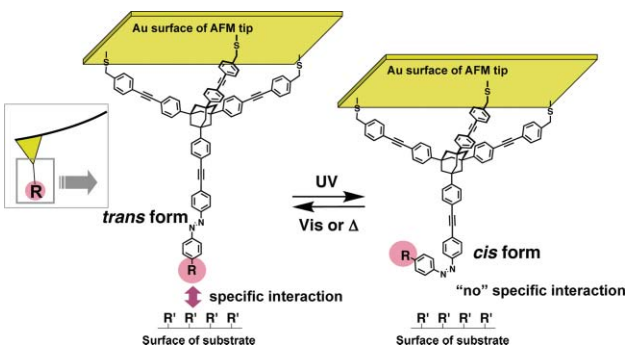

Fig. 1 Design of the photoswitching molecular tip. In the *trans* configuration, the tip apex with a functional group (**R**) will interact with specific functional groups (**R′**) on the substrate surface to provide chemical information. In the *cis* configuration, the tip apex does not present the functional group for specific chemical interactions with the substrate surface and provides only topographical information.

[a]*Department of Chemistry, Graduate School of Science, Tokyo Institute of Technology, 2-12-1 Ookayama, Meguro-ku, Tokyo 152-8551, Japan*
[b]*Department of Materials Engineering Science, Graduate School of Engineering Science, Osaka University, 1-3 Machikaneyama, Toyonaka, Osaka 560-8531, Japan. E-mail: kfukui@chem.es.osaka-u.ac.jp; Fax: +81 6 6850 6235*
[c]*Department of Radiology and Department of Chemistry, University of Pennsylvania, 231 South 34th Street, Philadelphia, PA 19104-6323, USA; Fax: +1 215 573 2112; Tel: +1 215 898 3105. E-mail: Yoko.Yamakoshi@uphs.upenn.edu, yamakoshi@org.chem.ethz.ch*
[d]*PRESTO, Japan Science and Technology Agency, 4-1-8 Honcho Kawaguchi, Saitama 332-0012, Japan*
† Electronic supplementary information (ESI) available: Further experimental details and characterisation data. See DOI: 10.1039/c002657c

change of the configuration of the molecule. We have chosen the azobenzene group since it is one of the most well studied photoswitching groups, converting between the thermodynamically favoured *trans*-form and the *cis*-form, which is usually obtained by UV light irradiation. As shown in Fig. 1, we expected that the *trans*-form of the molecular tip will probe the chemical property of the surface by the specific intermolecular interaction between the functional group (**R**) on the molecular tip and the other functional group (**R′**) on the surface. In contrast, the molecular tip with the *cis*-form can be used as a simple molecular tip for topographical imaging where no specific interaction is involved (Fig. 1). As the configurational change of the azobenzene moiety is generally reversible, we expected that we could switch the molecular tips simply by light irradiation of specific wavelengths, even during the measurement with the light source directly connected to NC-AFM machine. This approach makes possible the simultaneous measurement of topographical and chemical properties of a surface.

In our previous communication, we reported on the AFM studies of our first tripod (molecular tip **A** in the present report), which exhibits photoinduced configurational change.[12] We now present a full account of our studies on the syntheses of two photoswitching tripodal molecular tips, **A** and **B**, methods for immobilization of them onto the gold surface, and detection of photoinduced configurational change by NC-AFM imaging.

Results and discussion

Syntheses of tripodal molecules 13 and 14

Two tripodal molecules **A** and **B** (Scheme 3) respectively with a TMS acetylene and a carboxylic acid on the apex of the molecule were designed as photoswitching molecular tips. Molecular tip **A** was prepared as a model photoswitching tip and **B** was prepared as a molecular tip with a functional group (COOH) for chemical detection. The acetate precursors **13** and **14** were synthesized by a convergent synthesis involving the separate preparation of each key component (the core **2**, the leg **3**, and the apex **8** or **12**) and their subsequent conjugations (Schemes 1–3). The acetylene leg **3** was synthesized by a slightly modified literature procedure.[13,14] The 1,3,5,7-tetrakis(4-iodophenyl)adamantane **1** was prepared from 1-bromoadamantane according to the reports by Keana and co-workers,[6,7] and was converted to **2** by the single addition of a TMS acetylene group *via* a Sonogashira coupling controlled stoichiometrically (Scheme 1). The remaining three iodophenyl groups in **2** were subsequently substituted with the acetylene leg **3** under Sonogashira conditions. As noted also by Keana and co-workers,[6,7] a significantly low yield (20%) was observed in this Sonogashira coupling, presumably due to the interaction of the sulfur and the palladium catalyst. Therefore, high catalyst loading and an excess amount of alkyne **3** were required to yield usable amounts of product **4**. The core–legs conjugate **4** was subsequently subjected to deprotection conditions to give tripodal scaffold **5** with a single terminal alkyne (Scheme 1) that is available for further functionalization with an apex part.

Two azobenzene apexes **8** and **12**, respectively, for molecular tips **A** and **B** were synthesized as shown in Scheme 2. Apex **8** was prepared by an oxidative homocoupling[15] of aniline **6** and a subsequent Sonogashira coupling with TMS acetylene (TMSA).

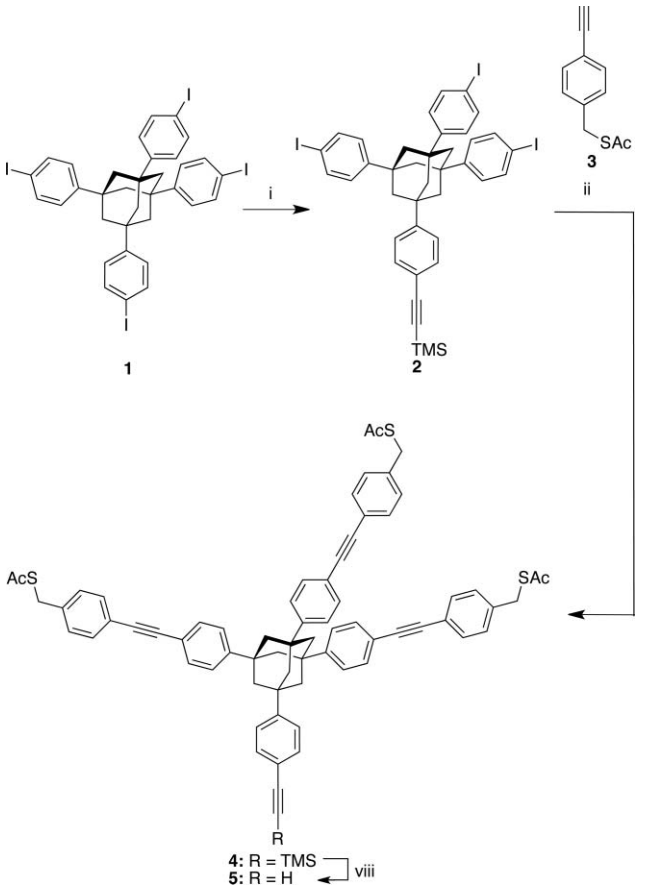

Scheme 1 Synthesis of the phenylacetylene–adamantane scaffold part (**5**) of tripodal molecular tips. Reagents and conditions: (i) TMSA, $Pd(PPh_3)_2Cl_2$, PPh_3, Et_3N, CuI, THF, reflux, 4 d, 85%; (ii) $Pd(PPh_3)_2Cl_2$, PPh_3, CuI, Et_3N, THF, reflux, 5 d, 20%; (iii) Bu_4NF, THF, –20 °C, 30 min, 56%.

Apex **12** was prepared by a hetero-coupling of an aniline and a nitrosophenyl derivative **11**.[16,17] Other conditions attempted for this hetero-coupling gave lower yields.[18]

The photoswitching tripods **13** and **14** were prepared by a Sonogashira coupling of azobenzene apex **8** or **12** with a terminal alkyne group of tripodal scaffold **5**. The reaction of acetylene **5** and aryl bromide **8** proceeded only in low yield (8%), presumably due to the interaction of sulfur and the Pd catalyst. In the preparation of **14**, where the more reactive aryl iodide **12** was used, a higher yield (48%) was obtained in shorter reaction times.

Photoinduced configurational changes of azobenzene derivatives 8, 12, 13 and 14 in solution

The configurational changes of the azobenzene moiety of apexes **8** and **12** and tripods **13** and **14** were first examined in CH_2Cl_2 solution using UV–Vis absorption analyses. The thermodynamically favoured configuration of azobenzene is usually *trans*, which can be converted to the *cis*-form by UV irradiation. The corresponding UV–Vis spectra of these configurations generally show characteristic absorption peaks. A model test with the azobenzene **8** was carried out with UV (360 ± 10 nm) and visible light (450 ± 10 nm) irradiation (Fig. 2d). The spectrum with an absorption maximum at 350 nm, which was observed prior to the

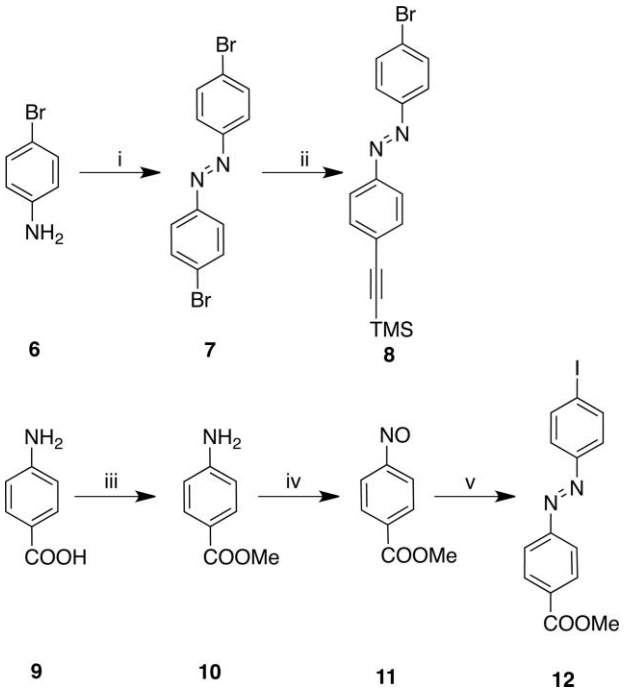

Scheme 2 Syntheses of the azobenzene apex parts (**8** and **12**) of molecular tips **A** and **B**. Reagents and conditions: (i) MnO_2, PhH, reflux, 4 h, 49%; (ii) TMSA, $Pd(PPh_3)_2Cl_2$, PPh_3, CuI, Et_3N, THF, reflux, 2 days, 48%; (iii) CH_3OH, c.H_2SO_4, reflux, 38 h, 93%; (iv) Oxone®, CH_2Cl_2, water, rt, 1 h, 95%; (v) 4-iodoaniline, acetic acid, rt, 1 d, 76%.

UV irradiation and after Vis irradiation, was assigned to be the *trans*-form (black line in Fig. 2d). The other spectrum, with an absorption maximum at 440 nm, which was obtained after UV irradiation, was assigned to be *cis* (red line in Fig. 2d), in good agreement to the spectra typically observed in many azobenzene derivatives. The same spectral changes in the other azobenzene apex **12** upon each light irradiation were also observed.[19]

UV–Vis spectra of azobenzene tripods **13** and **14** measured in CH_2Cl_2 solution are shown in Fig. 2a and b, respectively. In comparison to the spectra of tripod scaffold **5** (Fig. 2c), the largest

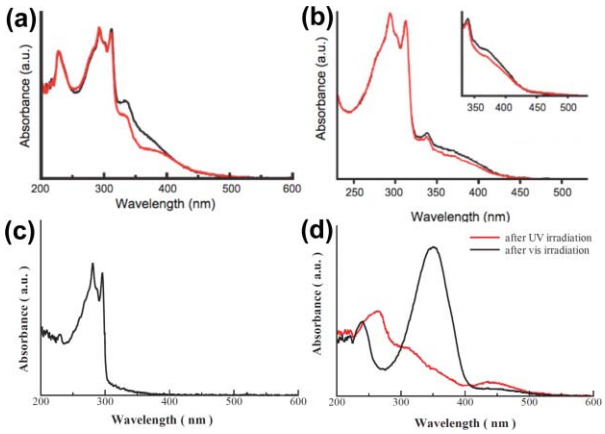

Fig. 2 UV–Vis spectra of tripods **13** (a), **14** (b), and **4** (c) and an azobenzene **8** (d) in CH_2Cl_2 solution. Black lines: the initial spectra or after visible light (450 ± 10 nm) irradiation. Red lines: the spectra after UV light (360 ± 10 nm) irradiation.

absorption peaks at 290 and 310 nm of **13** and **14** (Fig. 2a and 2b) are suggested to correspond to the tripodal adamantane–phenylacetylene skeleton. Upon irradiation with UV light (360 ± 10 nm), significant decreases in absorption peaks at around 340–400 nm for both **17** and **18** were observed. These peaks re-appeared upon visible light (450 ± 10 nm) irradiation. This absorption change was observed reversibly at least several times under light irradiation in a reproducible manner. These results suggested that the tripods **13** and **14** could change their configuration reversibly in solution phase and potentially can act as photoswitching molecular tips on gold under SPM conditions.

Optimizing the immobilization condition of thioacetate tripod onto gold substrate using tripodal scaffold 4

Since the thiol groups are known to be unstable towards oxidation, the simultaneous conversion from thioacetate to thiol and binding to the gold substrate was thought to be ideal as an immobilization method for molecular tips.[20–22] We planned to optimize the conditions for this deprotection/immobilization process using

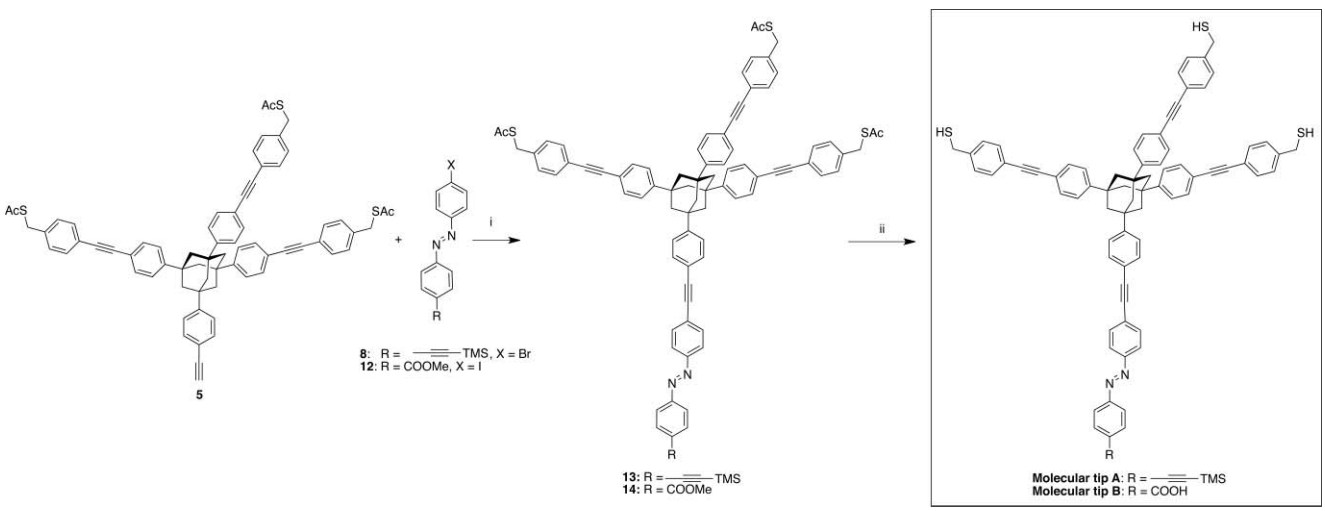

Scheme 3 Conjugations of tripodal scaffold and apex parts. Reagents and conditions: (i) $Pd(PPh_3)_2Cl_2$, PPh_3, CuI, Et_3N, THF, reflux, 4 d (for **13**) or 2 d (for **14**), 8% (for **13**) and 48% (for **14**); (ii) NH_4OH, THF (for **A**), NaOH, MeOH, THF, reflux, 2 h (for **B**).

compound **4**, which possesses the same tripodal scaffold with three terminal thioacetate groups as **13** and **14**. Also, molecule **4** is shorter than both of **13** and **14**, and thus was expected to be conductive enough for the subsequent STM scanning to visualize the immobilized molecules on the gold surface. To optimize the condition for immobilization, three methods (*methods A–C*) were conducted as follows. In *method A*, the gold substrate was soaked in a THF solution of **4** (0.1 μM) for 3 min. In *method B*, the gold substrate was soaked in a THF solution of **4** (0.1 μM, 2 mL) in the presence of aqueous NH_4OH solution (60 μL) for 3 min and subsequently rinsed with THF. In *method C*, the same conditions as *method B* were applied with additional thorough washing with water. The STM images of the gold substrates prepared under these conditions are shown in Fig. 3. All of the substrates were observed as the single crystal Au(111) surface of delineated terrace structure with discrete widths. As shown in Fig. 3a, the gold surface soaked simply in THF solution of **4** (*method A*) gave the image of the surface fully covered with small particles but no obvious structure whose size could be assigned to **4**. The STM image of the gold surface prepared in the presence of base (*method B*) shows the larger particles with diameters of 5–10 nm in addition to the smaller particles (Fig. 3b). By additional thorough washing with water (*method C*), this surface gave the STM image of Fig. 3c. Although most of the particles disappeared, the larger ones with *ca.* 5 nm diameter were still clearly observed. Since the size of these larger particles can correspond to the size of tripodal molecule, it was deduced that the tripodal molecules could be immobilized strongly on the gold surface by *method C*. The immobilized molecules were observed as single molecules and in a dispersed manner, which is appropriate as single molecular tip when immobilized on the gold AFM tip apex.

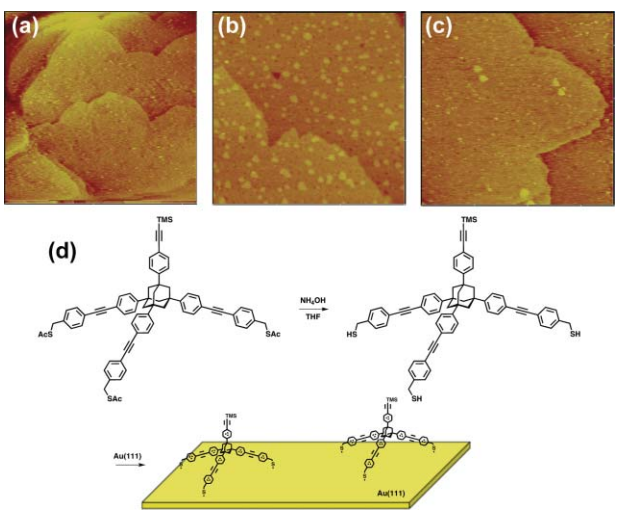

Fig. 3 STM imaging of the Au(111) surface with tripodal molecule **4**. ($V_s = -1.5$ V, $I_t = 0.3$ nA). (a) Soaked in 0.1 μM solution of **4** in THF (125 × 125 nm^2) (*method A*), (b) soaked in 0.1 μM solution of **4** in THF in the presence of NH_4OH and subsequently rinsed with THF (150 × 150 nm^2) (*method B*), (c) same as *method B*, with subsequent wash by water (150 × 150 nm^2) (*method C*). (d) Schematic illustration of *in situ* deprotection/immobilization of tripodal thioacetate molecule **4** on the gold surface. (Note that the paired particles in Fig. 3c are an artifact, as is obvious from the fact that all three pairs have the same intradistance and direction. The step edges are also observed as a duplicate image with similar separation. This is probably due to double probe apex of the STM tip used for imaging.)

NC-AFM imaging of tripodal molecular tip A

NC-AFM imaging of tripod **A** on a gold surface was carried out under ultra high vacuum (UHV) conditions. Based on the optimized conditions using scaffold **4**, tripod **A** was immobilized under *condition C* and the surface was dried subsequently under an UHV condition. The baking of the whole AFM machine was carried out to remove water that is naturally adsorbed on the surface and often disturbs the stable NC-AFM measurement. As shown in Fig. 4a and b, relatively larger and stationary particles (10–20 nm) were observed at least during the several times of the scanning interval. Interestingly, all of the particles show the same pattern and are in the diameter range of about 10–20 nm, which corresponds to the shape and the size of the AFM tip. This result suggested that the image of the tripod molecule is a reflection of the larger AFM tip. That is to say, since the molecular tip **A** was sharper than the AFM tip, the bigger object (AFM tip) was observed as an image (Fig. 4d). Taken together with our other recent results on other tripod molecular tips for ligand–receptor unbinding force measurement demonstrating that the tripodal structure provides high robustness to the molecular tip in comparison to the monopod SAM system,[23] this photoswitching tripod **A** is robust enough under UHV-NC-AFM imaging conditions and is suitable for stable AFM measurements.

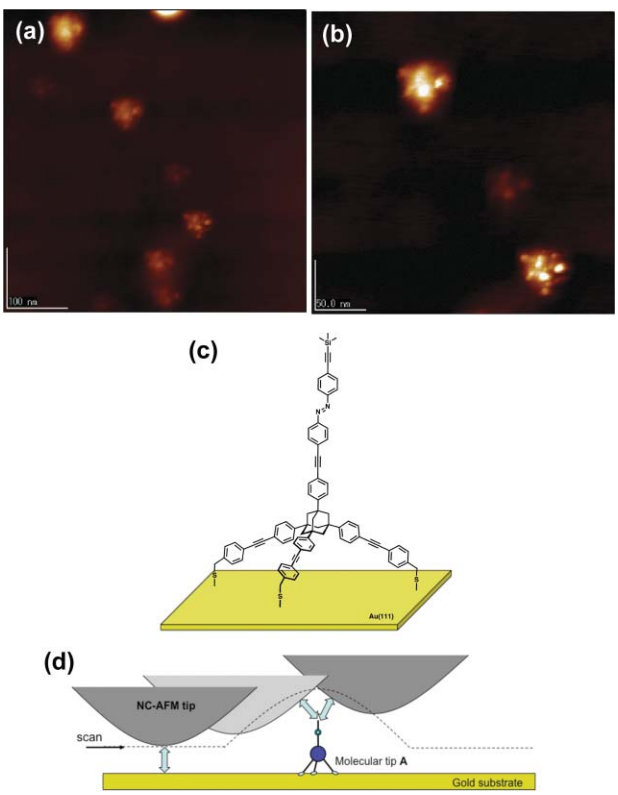

Fig. 4 UHV-NC-AFM imaging of molecular tip **A** immobilized on gold surface. $V_s = -0.4$ V, $D_f = -72$ Hz, $A_{p\text{-}p} = 12$ nm. (a) 480 × 480 nm^2, (b) 300 × 300 nm^2. (c) Structure of immobilized molecular tip **A**. (d) Illustration of the imaging of AFM tip by molecular tip **A**.

By extensive NC-AFM imaging of **A** on the gold surface, several kinds of images with different heights were observed, as previously reported.[24] The images with lower height were identified as flattened structures presumably due to the incomplete deprotection of the three thioacetate groups. Thus, for the attachment of molecular tip **B**, the final product with deprotected thiols was purified by extraction prior to the reaction with the gold surface.

NC-AFM imaging of molecular tip B on gold substrate

The preparation of **B** by complete deprotection of **14** was carefully carried out. The reaction progress was monitored by TLC, ^{1}H-NMR, and MALDI-TOF-MS to ensure the complete deprotection of all three thioacetates and one methylester. An aliquot of obtained **B** was dissolved in CH_2Cl_2 (0.2 μM). A clean Au(111) substrate was immersed in this solution for 3 min and immediately rinsed with CH_2Cl_2 to wash away the unbound molecules. The surface was subsequently subjected to UHV-NC-AFM imaging. Fig. 5 shows a typical NC-AFM image of molecular tip **B** adsorbed on the Au(111) surface. Imaging was carried out using a normal Au-coated cantilever. Isolated bright protrusions were observed on the Au(111) terrace. Interestingly, no preference for step edges was observed and the molecules were stationary on the surface during NC-AFM measurements at room temperature for at least a few hours. The NC-AFM images were analyzed in detail as follows.

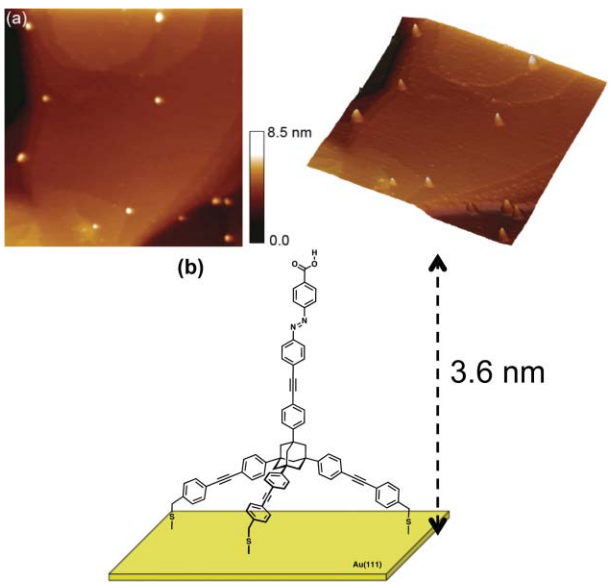

Fig. 5 (a) UHV-NC-AFM image of tripod molecular tip **B** adsorbed on the Au(111) substrate (610×610 nm^2, $\Delta f = -20$ Hz). The bright protrusions with an apparent height of 3.2 ± 0.1 nm were observed. Right panel is 3D view of the corresponding NC-AFM image. (b) Structure of immobilized molecular tip **B**.

Line profile analyses of the bright protrusions revealed that the molecules had an apparent height of 3.2 ± 0.1 nm. The diameters of the bright protrusions were observed to be larger than expected due to the convolution of the tip shape with a typical effective apex radius of 50 nm (Fig. 5a). From the molecular structure, the physical topography of molecular tip **B** in the *trans* configuration with upright form on the gold surface (Fig. 5b) was estimated to be about 3.6 nm by MM2 calculation, providing a slightly higher value than the observed height. This observation might be explained as follows. It has been noted that the force between a tip and a substrate can be reflected in the frequency shift of NC-AFM measurement, which is the sum of the forces working between the tip apex and surface.[25] When the tip passes above a tall molecule, in contrast to the flat Au(111) surface, the AFM tip is pulled up to compensate for the increased force originating from the tall molecule. Forces between a lifted tip and the surrounding Au surface are reduced due to the increased tip–surface distance. The feedback regulation pushes the tip down to restore the lost forces.[26] A similar phenomenon was observed in the measurement of molecular tip **A** on Au(111),[12,25] but to a lesser extent due to the relatively bulky top (TMS) of **A**.

Another possible assignment of the observed height for the protrusions is tripod **B** in the *cis* configuration. However, the physical topography of a *cis*-**B** standing upright on the Au surface is estimated to be *ca.* 3.0 nm. The presence of electrostatic force generally can be the only reason to provide a smaller observed height value than the estimation, and the electric dipole of the *cis*-**B** can not be large enough to explain this height difference. In addition, general photoisomerization energies of azobenzene in the gas phase are 3.55 eV (UV light; $\lambda \sim 350$ nm) and 2.82 eV (visible light; $\lambda \sim 440$ nm) between the *trans*-form and the *cis*-form.[27] As described above, the UV–Vis spectra of molecule **18** in the solution phase shows that the initial configuration of **18** is all *trans* and the *cis*-form produced by irradiation of UV light gradually converted to the *trans*-form even at room temperature. Taken together, we assigned the bright protrusions in Fig. 5 to single molecules of *trans*-**B** adsorbed on Au(111) in an upright form.

In our previous communications, we have carried out the imaging of molecular tip **A** immobilized by *method C* by NC-AFM and gave two kinds of images with heights of 3.7 ± 0.3 nm and less than 2.5 nm.[12,25] We concluded that the former image corresponded to the molecular tip **A** standing upright on the tripod scaffold, and the latter to molecule **A** flattened on the gold surface. We speculated that these images with shorter height appeared due to the incomplete deprotection of the three thioacetate groups. In the present study, only the images with 3.2 ± 0.1 nm were observed, indicating successful immobilization of molecular tip **B** on the gold surface by the complete deprotection of the three thioacetates in the tripod legs.

As described above, the immobilized molecular tip **B** did not move on the gold surface even over several hours at room temperature. Achievement of this stable immobilization is possibly due to three S–Au covalent bonds. The mobility of thiol derivatives on gold substrates was previously reported. The insertion of a molecule with a terminal thiol group into the alkanethiol SAM matrix was observed by STM as a potential molecular wire.[28–30] However, the mobility of such thiol molecules was reported to be very fast. For example, 4-biphenylmethanethiol (BMT) inserted in a SAM of bicyclo[2.2.2]octane derivative (BCO) was imaged by STM and showed that the location of isolated BMT rapidly changed as a function of time at room temperature, even when the BCO–SAM is formed in a highly ordered manner.[31] Thermal diffusion was thought to be the major reason because such mobility was lost at 110 K.[32] Further investigations are necessary to clarify the actual reason for the difference in mobility, which

should be important for technological application of SAM-based nanostructures.

Photoisomerization behaviour of molecular tip B on Au(111) surface

The photoinduced isomerization of molecular tip **B** on a Au(111) surface was examined by focusing on analysis of individual molecules at the single molecular level. Following the initial imaging of a single *trans*-**B** molecule carried out by NC-AFM, the surface was irradiated by UV light (360 ± 10 nm) for 10 min while the tip was retracted from the surface at a distance of *ca.* 1.3 μm. Immediately after, the identical molecule was scanned by NC-AFM again. The initial bright protrusions in Fig. 6b were assigned to the *trans*-**B** molecule standing upright on the Au surface on the tripod scaffold, which were converted to the one with a decreased height by about 0.4 nm. The apparent height of the molecules recovered to the initial value by subsequent irradiation of visible light (450 ± 10 nm). As results from the observation of several single molecules, the changes in the apparent height of the molecule by UV and visible light irradiation falls into the range of 0.4 ± 0.1 nm. These results indicate that the reversible *trans*–*cis* configurational change occurs by the photoirradiation on the gold surface under UHV conditions. The same photoswitching behaviour of molecular tip **B** was also observed in air (data is not shown).

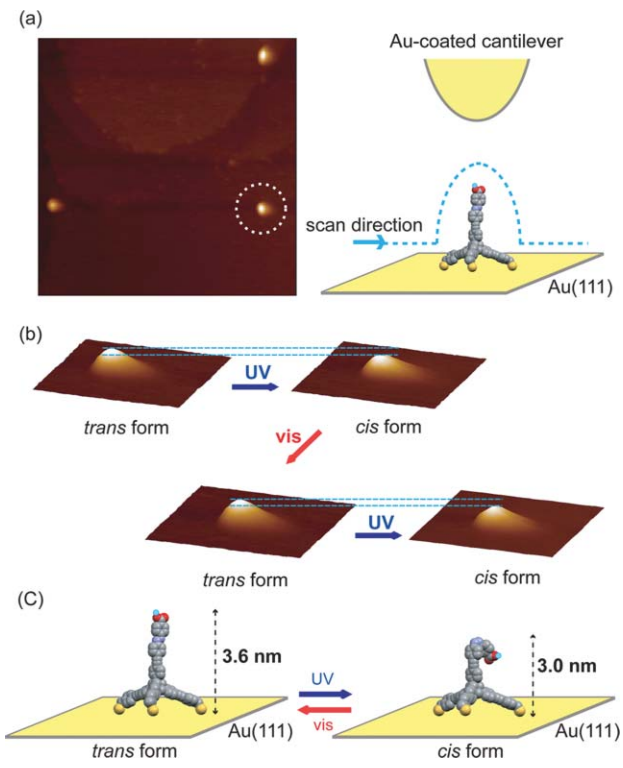

Fig. 6 (a) UHV-NC-AFM image (350 × 350 nm^2, Δf = −28 Hz) of molecule **B** adsorbed on Au(111) using a Au-coated cantilever and schematic of the measurement. (b) A series of 3D view of NC-AFM images (55 × 55 nm^2, Δf = −28 Hz) of a **B** adsorbed on Au(111), which was indicated by a white circle in (a) representing the *trans* form (after visible light (450 ± 10 nm) irradiation) and the *cis* form (after UV light (360 ± 10 nm) irradiation) and corresponding line profiles are indicated. (c) Molecular models of **B** fixed on the Au substrate in *trans* and *cis* configurations.

The observed height difference (0.4 ± 0.1 nm) was smaller than the estimated value (0.6 nm) from the physical topography of both *trans*- and *cis*-**B** (Fig. 6c). As described above, the isolated tall molecules observed by NC-AFM can show shorter height than the physical estimation to compensate for the sudden decrease of van der Waals force from the substrate. The experimentally obtained results were consistent with this interpretation; the observed height of 3.2 ± 0.1 nm is lower than the estimated physical topography (*ca.* 3.6 nm) of *trans*-**B**, and the observed height of 2.8 ± 0.1 nm is lower than the estimated one (*ca.* 3.0 nm) of *cis*-**B**. The tip is closer to the substrate when it traces the top of the *cis*-form and the atom density at the apex of the molecule is higher for the *cis*-form. These two factors can increase the van der Waals attraction compared to the case of the *trans* isomer.

It has been known that the photoexcited state of photoswitching molecules such as azobenzenes and diarylethenes can be easily quenched by Au surfaces *via* photoinduced electron transfer,[33,34] as observed by STM imaging. Therefore, many efforts have been taken to have more distance or to add SAM scaffold with less propensity for electron transfer between the photoreactive moiety and the gold surface.[35] In this study, the photoinduced isomerization occurred in a quantitative yield on the gold surface, indicating that the location of the azobenzene moiety was far enough from the gold surface without conductive linkage of the molecules.

In our previous report, we have attached molecular tip **A** on the gold-coated AFM tip surface and carried out the scanning of the Au(111) surface to detect the photoswitching property of the single molecular tip.[12] Currently, further efforts on the attachment of molecular tip **B**, which possess the carboxylic group on the apex as a chemical identification probe, and detection of the intermolecular interactions of the functional surface are in progress.

Conclusions

Two tripodal molecules **A** and **B** were designed and synthesized as photoswitching single molecular tips for the purpose of AFM tip functionalization. They were prepared by multi-step organic synthesis and were applied to the immobilization onto a Au(111) surface for single molecular analysis of the photoisomerization. A base-promoted *in situ* deprotection and immobilization of **A** was successfully carried out on the Au(111) surface and adsorbed single molecules were observed to be spatially isolated by UHV-NC-AFM imaging. In the case of molecular tip **B**, complete deprotection and purification of the molecule was carried out prior to the reaction with gold. A single molecule of **B** on the Au(111) surface was analyzed by UHV-NC-AFM imaging after photoirradiation treatments with UV (360 ± 10 nm) and visible light (450 ± 10 nm). The reversible changes of the height of **B**, which correspond to the *trans*- and the *cis*-isomers, were confirmed. Taken together with the fact that the adsorbed molecule was stationary on the surface for hours at room temperature, these adsorbed tripodal molecular tips can serve for both topographical and chemical imaging of a surface under NC-AFM conditions.

Experimental

General

Melting points were recorded on a melting point apparatus MP-21 (Yamato Scientific Co., Ltd., Tokyo, Japan) using open capillary tubes and remain uncorrected. The ^{1}H- and ^{13}C-NMR spectra were recorded on a Mercury plus 400 (Varian Inc., CA, USA) at 400 MHz for ^{1}H and 125 MHz for ^{13}C, and in $CDCl_3$ (Merck KGaA, Darmstadt, Germany) unless otherwise noted. Chemical shifts are expressed in δ units (ppm) with the residual solvent peaks (^{1}H $CHCl_3$, δ 7.26; ^{13}C $CHCl_3$, δ 77.0) as internal standards. Coupling constants (J) are reported in Hertz (Hz). Mass spectra obtained *via* FAB-MS and MALDI-TOF-MS were recorded respectively on a JMS-700 (JEOL Ltd., Tokyo, Japan) and an AB4700 (Applied Biosystems Japan Ltd., Tokyo, Japan) or a Bruker MALDI-TOF-TOF (Bruker, Billerica, MA, USA). IR spectra were recorded on an FT/IR-460 plus (JASCO Co., Tokyo, Japan). UV–Vis absorption spectra were recorded in CH_2Cl_2 on a UV-265 (SHIMADZU Co., Kyoto, Japan). Column chromatography and preparative thin-layer chromatography (TLC) were carried out on silica gel Wakogel® C-200 (200 mesh, Wako Pure Chemical Industries, Ltd.) and on silica plate Partisil® PK6F (16.0 nm, layer thickness 1000 µm, Whatman plc, Middlesex, UK), respectively. Analytical TLC was performed on commercially coated plastic plates Silica gel 60 mesh F_{254}, (Merck KgaA). Spots were rendered visible by exposing the plate to UV light. All reagents were purchased from commercial suppliers as described and used without further purification. Tetrahydrofuran (99.5%, anhydrous, inhibitor free, Kanto Chemical Co., Inc., Tokyo, Japan), triethylamine, dichloromethane, diethyl ether (Wako Pure Chemical Industries, Ltd., Osaka, Japan), and other reagent-grade solvents (chloroform, methanol, benzene, hexane, Kanto Chemical Co., Inc.) were used as received. Brine refers to saturated aqueous solution of NaCl.

Trimethyl[4-[3,5,7-tris(4-iodophenyl)adamantan-1-yl]phenylethynyl]silane (2)

A mixture of 1,3,5,7-tetrakis(4-iodophenyl)adamantane **1** (0.54 g, 0.6 mmol), $Pd(PPh_3)_2Cl_2$ (9.0 mg, 0.01 mmol), and PPh_3 (1.7 mg, 0.006 mmol) was placed in a Schlenk flask, degassed, and replaced with Ar gas. The evacuation and flushing process was repeated three times. THF (10 ml), TMSA (55 µl, 0.39 mmol), and Et_3N (72 µl, 0.39 mmol) were added to the mixture above in succession by gastight syringes. After repetition of freeze-pump-thaw for three times, CuI (0.6 mg, 0.003 mmol) was added. The flask was immersed in a thermostated oil bath and refluxed for 4 days. The reaction mixture was poured into water and extracted with CH_2Cl_2. The combined organic extracts were washed with brine, dried over anhydrous $MgSO_4$, and concentrated *in vacuo*. The resulting yellow oil was purified by silica gel chromatography with hexane–EtOAc (10 : 1) to give a yellow solid **2** (0.45 g, 85%): R_f 0.9 (hexane–EtOAc (5 : 1)); mp 152–154 °C; ^{1}H NMR (400 MHz, $CDCl_3$) δ 0.25 (s, 9H, TMS), 2.06 (s, 12H, adamantane C**H$_2$**), 7.19 (d, J = 8.6 Hz, 6H, Ar**H**), 7.37 (d, J = 8.6 Hz, 2H, Ar**H**), 7.45 (d, J = 8.6 Hz, 2H, Ar**H**), 7.67 (d, J = 8.8 Hz, 6H, Ar**H**); ^{13}C NMR (125 MHz, $CDCl_3$) δ –0.0 (–TMS), 39.0 (adamantane C**H$_2$**), 46.7 (adamantane quaternary **C**), 90.9 (Ph–**C**≡), 91.7 (Ph**C** adjunct to I), 105.8 (≡**C**–TMS), 124.6 (Ph**C**), 127.1 (Ph**C**), 127.1 (Ph**C**H *ortho* or *meta* to I), 128.9 (Ph**C**), 132.1 (Ph**C**), 137.5 (Ph**C**H *ortho* or *meta* to I), 148.4 (Ph**C** *para* to I); FT-IR (KBr, cm^{-1}); 2927(m), 2896(m), 2851(m), 2156(w), 1485(s), 1390(w), 1355(w), 1247(s), 1187(w), 1067(w), 1002(s), 862(s), 842(s), 777(m), 756(m), 696(w), 647(w); MS (FAB) m/z 915 ([M+H]$^+$); Anal. Calcd for $C_{39}H_{37}I_3Si$: C, 51.22; H, 4.08; Found: C, 51.04; H, 4.24.

Trimethyl[4-[3,5,7-tris-[4-(4-acetylsulfanylmethylphenylethyny]-phenyl]adamantan-1-yl]phenylethynyl]silane (4)

To a mixture of **2** (0.38 g, 0.4 mmol), $Pd(PPh_3)_2Cl_2$ (53.6 mg, 0.08 mmol), and PPh_3 (10 mg, 0.04 mmol) in a Schlenk flask, THF (20 mL) was added. The solution was degassed by freeze-pump-thaw three times. After the addition of **3** (44 mg, 2.3 mmol), Et_3N (427 µl, 2.3 mmol) was added in succession by a gastight syringe. After repetition of the freeze-pump-thaw for an additional three times, CuI (3.5 mg, 0.02 mmol) was added. The flask was immersed in a thermostated oil bath and refluxed for 5 days. The reaction mixture was poured into water and extracted with CH_2Cl_2. The combined organic extracts were washed with brine, dried over anhydrous $MgSO_4$, and concentrated *in vacuo*. The resulting red-brown oil was purified by silica gel column chromatography with hexane–CH_2Cl_2 (1 : 10) to give yellow crystals **4** (79 mg, 20%): R_f 0.3 (hexane–EtOAc (2 : 1)); mp 118–120 °C; ^{1}H NMR (400 MHz, $CDCl_3$) δ 0.25 (s, 9H, –C**H$_3$** in TMS), 2.16 (brs, 12H, –C**H$_2$**– in adamantane), 2.36 (s, 9H, –C**H$_3$** in SAc), 4.12 (s, 6H, –C**H$_2$**–SAc), 7.2–7.4 (m, 4H, Ar**H**), 7.4–7.6 (m, 24H, Ar**H**); ^{13}C NMR (125 MHz, $CDCl_3$) δ –0.0 (TMS), 30.3 (–**C**H$_3$, in SAc), 33.3 (–**C**H$_2$–SAc), 39.3 (–**C**H$_2$– in adamantane), 46.8 (quaternary **C** in adamantane), 88.9 (–**C**≡C–), 89.5 (–**C**≡C–), 94.2 (Ph–**C**≡), 105.5 (≡**C**–TMS), 121.1 (Ph**C**), 122.3 (Ph**C**), 124.9 (Ph**C**), 125.1 (Ph**C**), 125.1 (Ph**C**H), 128.8 (Ph**C**H), 131.7 (Ph**C**H), 131.8 (Ph**C**H), 132.0 (Ph**C**), 137.8 (Ph**C**), 149.2 (Ph**C**), 149.4 (Ph**C**), 195.0 (**C**=O); FT-IR (KBr, cm^{-1}); 2924(m), 2850(w), 2211(w), 2154(w), 1686(s), 1509(m), 1411(w), 1353(m), 1246(w), 1132(m), 1101(w), 1018(m), 958(m), 833(s), 775(w), 699(w), 626(m). MS (FAB) m/z 1101 ([M+H]$^+$); Anal. Calcd for $C_{72}H_{64}O_3S_3Si$: C, 78.50, H, 5.86; S, 8.73. Found: C, 78.75; H, 5.81; S, 8.60; UV–Vis (in CH_2Cl_2, λ_{max}, nm): 290 nm, 310 nm.

4-[3,5,7-Tris-[4-(4-acetylsulfanylmethylphenylethynyl)phenyl]-adamantan-1-yl]phenylethyne (5)

A 1.0 M solution of Bu_4NF (30.2 mg, 0.1 mmol) in THF (0.1 mL) was added to a stirred solution of **4** (96 mg, 0.09 mmol) in THF (10 mL) at –20 °C dropwise over 30 min. The solution was subsequently stirred for 30 min at –20 °C under Ar atmosphere. The reaction mixture was poured into water and extracted with CH_2Cl_2. The combined organic extracts were washed with brine, dried over anhydrous $MgSO_4$, and concentrated *in vacuo*. The resulting orange oil was purified by silica gel column chromatography with hexane–CH_2Cl_2 (1 : 10) to give a yellow solid **5** (50 mg, 56%): R_f 0.2 (hexane–EtOAc (2 : 1)); ^{1}H NMR (400 MHz, $CDCl_3$) δ 2.16 (s, 12H, –C**H$_2$**– in adamantane), 2.36 (s, 9H, –C**H$_3$** in SAc), 3.06 (s, 1H, ≡C**H**), 4.12 (s, 6H, –C**H$_2$**–SAc), 7.2-7.4 (m, 4H, Ar**H**), 7.4-7.6 (m, 24H, Ar**H**); FT-IR (KBr, cm^{-1}); 2924(m), 2850(w), 2211(w), 1686(s), 1509(s), 1354(m), 1238(w), 1131(m), 1099(m), 1017(m), 956(m), 831(s), 773(m), 698(w), 624(s); MS (MALDI-TOF) m/z 1028 (M$^+$).

(*E*)-1,2-Bis(4-bromophenyl)diazene (7)[15]

A solution of 4-bromo aniline (**6**, 2.58 g, 15 mmol, Wako Pure Chemical Industries, Ltd.) and dried active manganese(IV) oxide (MnO_2, 99.5%, 6.52 g, 75 mmol, Wako Pure Chemical Industries, Ltd.) in anhydrous benzene (120 mL) was refluxed for 4 h with a Dean–Stark apparatus. The reaction mixture was filtered in hot and the manganese oxide washed with benzene. The filtrate was concentrated *in vacuo* and the resulting red-purple crystals were purified by silica gel column chromatography with hexane–CH_2Cl_2 (10 : 1) to give orange crystals **7** (1.27 g, 49%): R_f 0.8 (hexanes–EtOAc (2 : 1)); mp 203–205 °C; ^{1}H NMR (400 MHz, $CDCl_3$) δ 7.66 (d, J = 8.8 Hz, 4H, Ar**H**), 7.80 (d, J = 8.9 Hz, 4H, Ar**H**); FT-IR (KBr, cm^{-1}); 2927(w), 1654(m), 1389(w), 1280(w), 1153(w), 1096(w), 1064(s), 1005(m), 835(s), 710(w), 634(w), 537(m), 459(m); MS (MALDI-TOF-MS) m/z 339 (M^+); Anal. Calcd for $C_{12}H_8N_2Br_2$: C, 42.39; H, 2.37; N, 8.24. Found: C, 42.66; H, 2.33; N, 8.35.

(*E*)-1-(4-Bromophenyl)-2-[4-[(trimethylsilyl)ethynyl]phenyl]-diazene (8)

A solution of **7** (1.18 g, 3.5 mmol), $Pd(PPh_3)_2Cl_2$ (72.7 mg, 0.1 mmol), and PPh_3 (13.5 mg, 0.05 mmol) in THF (20 ml) was degassed by freeze-pump-thaw for three times in a Schlenk flask. Subsequently, TMSA (441 µl, 3.1 mmol) and Et_3N (578 µl, 3.1 mmol) were added in succession by gastight syringes. After repetition of the freeze-pump-thaw process three times, CuI (4.8 mg, 0.025 mmol) was added. The flask was immersed in a thermostated oil bath, and refluxed for 2 days. The reaction mixture was poured into water and extracted with CH_2Cl_2. The combined organic extracts were washed with brine, dried over anhydrous $MgSO_4$, and concentrated *in vacuo*. The resulting purple solid was purified by silica gel column chromatography with hexane–EtOAc (10 : 1) to give a red-yellow solid (40 mg), which was purified by TLC with hexane–EtOAc (4 : 1) to a give orange solid **8** (20 mg, 48%): R_f 0.5 (hexane–EtOAc (2 : 1)); mp 120–122 °C; ^{1}H NMR (400 MHz, $CDCl_3$) δ 0.28 (s, 9H, –C**H**$_3$ in TMS), 7.61 (d, J = 8.8 Hz, 2H, Ar**H**), 7.66 (d, J = 8.8 Hz, 2H, Ar**H**), 7.80 (d, J = 8.8 Hz, 2H, Ar**H**), 7.86 (d, J = 8.8 Hz, 2H, Ar**H**); ^{13}C NMR (400 MHz, $CDCl_3$) δ –0.1 (TMS), 97.4 (–**C**≡C–), 104.5 (–**C**≡C–), 122.9 (Ph**C**H), 124.4 (Ph**C**H), 125.7 (Ph**C**), 126.1 (Ph**C**), 132.4 (Ph**C**H), 132.8 (Ph**C**H), 151.3 (Ph**C** adjunct to N), 151.7 (Ph**C** adjunct to N); FT-IR (KBr, cm^{-1}); 2957(m), 2156(m), 1475(m), 1398(m), 1252(m), 1226(m), 1153(w), 1099(w), 1064(m), 1006(m), 848(s), 759(m), 633(w), 558(m); MS (FAB) m/z 356 (M^+), Anal. Calcd for $C_{17}H_{17}BrN_2Si$: C, 57.14; H, 4.80; N, 7.81. Found: C, 56.87; H, 4.80; N, 7.78. UV–Vis (in CH_2Cl_2, λ_{max}, nm): 450 nm, 350 nm.

Methyl-4-aminobenzoate (10)

To a solution of 4-aminobenzoic acid **9** (8.0 g, 58.3 mmol, Tokyo Chemical Industry CO., Ltd.) in methanol (150 mL), concentrated sulfuric acid (7 mL) was added slowly dropwise. The reaction mixture was refluxed for 38 h. The solution remaining was concentrated *in vacuo*. After the addition of water (100 mL), the pH was adjusted to 3 using 2 M NaOH. The precipitate formed was separated by filtration, and was washed with water (50 mL) to give a colourless solid **10** (8.23 g, 93%): R_f 0.5 (hexane–EtOAc (1 : 2)); ^{1}H NMR (400 MHz, $CDCl_3$) δ 3.85 (s, 3H, –C**H**$_3$), 4.05 (brs, 2H, –N**H**$_2$), 6.64 (d, J = 8.6 Hz, 2H, Ar**H** *ortho* to amine), 7.85 (d, J = 8.8 Hz, 2H, Ar**H** *meta* to amine).

Methyl-4-nitrosobenzoate (11)[16]

To a solution of **10** (2.5 g, 16.6 mmol) in 50 mL of CH_2Cl_2, an aqueous solution of Oxone® (20.3 g, 33.1 mmol, Wako Pure Chemical Industries, Ltd. in 200 mL of water) was added. The reaction mixture was stirred under Ar atmosphere at room temperature for 1 h. After separation of the two layers, the aqueous layer was extracted with CH_2Cl_2 twice. The combined organic layers were washed with 1 N HCl, saturated sodium bicarbonate solution, water, and brine, then dried over anhydrous $MgSO_4$ and concentrated *in vacuo* to dryness. The crude solid residue was recrystallized from CH_2Cl_2 to give a yellow solid **11** (2.58 g, 95%): R_f 0.3 (hexane–EtOAc (1 : 2)); mp 122–125 °C; ^{1}H NMR (400 MHz, $CDCl_3$) δ 3.98 (s, 3H, –C**H**$_3$), 7.94 (d, J = 8.8 Hz, 2H, Ar**H** *meta* to nitroso), 8.30 (d, J = 8.8 Hz, 2H, Ar**H**, *ortho* to nitroso); FT-IR (KBr, cm^{-1}); 3102(w), 3073(w), 2964(w), 1943(w), 1731(s), 1601(m), 1442(s), 1415(s), 1277(s), 1188(m), 1111(s), 1018(m), 962(m), 876(m), 845(m), 810(m), 766(s), 694(s), 659(w), 632(w), 540(w), 523(w), 455(w), 431(w).

(*E*)-Methyl 4-[(4-iodophenyl)diazenyl]benzoate (12)[17]

To a solution of **11** (0.6 g, 3.5 mmol) in 25 ml of acetic acid, 4-iodoaniline (0.6 g, 2.9 mmol) was added. The reaction mixture was stirred at room temperature for 24 h. The precipitate was separated by filtration, washed with water, and dried. The resulting orange solid (0.8 g) was purified by silica gel TLC with hexane–CH_2Cl_2 (1 : 4) to give red crystals **12** (760 mg, 76%): R_f 0.3 (hexane–CH_2Cl_2 (1 : 4)); mp 206–208 °C; ^{1}H NMR (400 MHz, $CDCl_3$) δ 3.96 (s, 3H, –C**H**$_3$), 7.61 (d, J = 8.6 Hz, 2H, Ar**H**), 7.82 (d, J = 8.6 Hz, 2H, Ar**H**), 7.88 (d, J = 8.6 Hz, 2H, Ar**H**), 8.12 (d, J = 8.6 Hz, 2H, Ar**H**); ^{13}C NMR (400 MHz, $CDCl_3$) δ 52.6 (–**C**H$_3$), 98.9 (Ph**C**), 122.99 (Ph**C**H), 124.90 (Ph**C**H), 130.89 (Ph**C**H), 132.31 (Ph**C**), 138.73 (Ph**C**H), 152.0 (Ph**C** adjunct to N), 155.1 (Ph**C** adjunct to N), 166.72 (**C**=O); FT-IR (KBr, cm^{-1}); 2926(m), 2852(s), 1718(s), 1279(s), 1192(w), 1144(w), 1111(m), 1054(m), 1002(m), 955(w), 864(m), 830(s), 805(m) 773(m), 710(w); MS(FAB) m/z 366 ([M]$^+$), HRMS; calcd for $C_{14}H_{11}IN_2O_2$, m/z 365.9865; Found: 365.9955; UV–Vis (in CH_2Cl_2, λ_{max}, nm): 445 nm, 340 nm.

(*E*)-1-[4-[3,5,7-Tris-[4-(4-acetylsulfanylmethylphenylethynyl)-phenyl]adamantan-1-yl]phenylethynyl]-2-[4-[(trimethylsilyl)-ethynyl]phenyl]diazene (13)

A solution of **5** (50 mg, 0.05 mmol), $Pd(PPh_3)_2Cl_2$ (5.7 mg, 0.008 mmol), and PPh_3 (1.0 mg, 0.004 mmol) in THF (30 mL) in a Schlenk flask was degassed by freeze-pump-thaw three times. After **8** (86 mg, 0.24 mmol) was added to the reaction mixture, Et_3N (45 µL, 0.24 mmol) was added in succession by a gastight syringe in Ar atmosphere. After repetition of the freeze-pump-thaw three times, CuI (0.3 mg, 0.002 mmol) was added. The flask was immersed in a thermostated oil bath and refluxed for 4 days. The reaction mixture was poured into water and extracted with CH_2Cl_2. The combined organic extracts were washed with brine, dried over anhydrous $MgSO_4$, and concentrated *in vacuo*. The resulting red-orange oil was purified by silica gel TLC with

hexane–CH_2Cl_2 (1 : 1) to give a red-yellow solid (40 mg), which was purified by additional TLC with hexane–EtOAc (2 : 1) to give a red solid **13** (5.2 mg, 8%): R_f 0.2 (hexane–EtOAc (2 : 1)); mp 108–110 °C; ^{1}H NMR (300 MHz, $CDCl_3$) δ 0.07 (s, 9H, –C**H**$_3$ in TMS), 2.16 (brs, 12H, –C**H**$_2$– in adamantane), 2.35 (s, 9H, –C**H**$_3$ in SAc), 4.05 (s, 6H, –C**H**$_2$–SAc), 7.2-7.4 (m, 4H, Ar**H**), 7.4-7.6 (m, 24H, Ar**H**), 7.68 (d, J = 8.1, 2H, Ar**H**), 7.71 (d, J = 8.1, 2H, Ar**H**), 7.72 (d, J = 8.6, 2H, Ar**H**), 7.87 (d, J = 8.6, 2H, Ar**H**); ^{13}C NMR (125 MHz, $CDCl_3$) δ –0.0 (TMS), 30.3 (–CH_3, in SAc), 33.3 (–CH_2–SAc), 39.4 (–CH_2– in adamantane), 46.9 (quaternary **C** in adamantane), 88.9 (–**C**≡C–), 89.5 (–**C**≡C–), 90.1 (–**C**≡C–), 97.2 (Ph–**C**≡), 105.5 (≡**C**–TMS), 121.1 (Ph**C**), 122.3 (Ph**C**), 124.9 (Ph**C**), 125.1 (Ph**C**), 125.1 (Ph**CH**), 128.5 (Ph**CH**), 128.8 (Ph**CH**), 129.2 (Ph**CH**), 129.2 (Ph**CH**), 131.0 (Ph**CH**), 131.7 (Ph**CH**), 131.8 (Ph**CH**), 132.0 (Ph**C**), 133.3 (Ph**CH**), 137.8 (Ph**C**), 148.9 (Ph**C**), 149.4 (Ph**C**), 195.0 (**C**=O); FT-IR (KBr, cm^{-1}); 2925(s), 2854(m), 2201(w), 1719(s), 1686(s), 1509(w), 1458(w), 1355(w), 1281(s), 1131(s), 1071(m), 1017(w), 958(w), 838(s), 774(w), 700(w), 626(m); MS(MALDI-TOF) m/z 1304 ([M]$^+$); UV-vis (in CH_2Cl_2, λ_{max}, nm) 290 nm, 310 nm, 335 nm, 390 nm.

4-[4-(4-{3,5,7-Tris-[4-(4-acetylsulfanylmethyl-phenylethynyl)-phenyl]-adamantan-1-yl}-phenylethynyl)-phenylazo]-benzoic acid methyl ester (14)

A solution of **5** (30 mg, 0.03 mmol), $Pd(PPh_3)_2Cl_2$ (3.0 mg, 0.004 mmol), and PPh_3 (0.5 mg, 0.002 mmol) in THF (15 ml) in a Schlenk flask was degassed by freeze-pump-thaw five times. After the addition of **12** (44 mg, 0.12 mmol), Et_3N (22 µl, 0.12 mmol) was added in succession by a gastight syringe. After repetition of the freeze-pump-thaw three times, CuI (0.3 mg, 0.002 mmol) was added. The flask was immersed in a thermostated oil bath and refluxed for 2 days. The reaction mixture was filtered and the residue was washed with CH_2Cl_2. The combined organic layers were concentrated *in vacuo*. The resulting red-orange solid (0.2 g) was purified by silica gel column chromatography with hexane–CH_2Cl_2 (1 : 9) to give orange crystals **14** (26 mg, 48%): R_f 0.3 (hexane–CH_2Cl_2 (1 : 9)); mp 132–135 °C; ^{1}H NMR (400 MHz, $CDCl_3$) δ 2.16 (brs, 12H, –C**H**$_2$– in adamantane), 2.36 (s, 9H, –C**H**$_3$ in SAc), 3.96 (s, 3H, –C**H**$_3$ in Me), 4.11 (s, 6H, –C**H**$_2$–SAc), 7.2–7.4 (m, 4H, Ar**H**), 7.4–7.7 (m, 24H, Ar**H**), 7.69 (d, J = 8.4 Hz, 2H), 7.85 (d, J = 8.4, 2H), 7.92 (d, J = 8.6, 2H), 8.17 (d, J = 8.6, 2H); ^{13}C NMR (125 MHz, $CDCl_3$) δ 30.6 (–CH_3, in SAc), 33.5 (–CH_2–SAc), 39.6 (–CH_2– in adamantane), 47.0 (quaternary **C** in adamantane), 49.5 (–CH_3, in Me), 84.9 (–**C**≡C–), 89.2 (–**C**≡C–), 89.7 (–**C**≡C–), 90.8 (–**C**≡C–), 121.4 (Ph**C**), 122.5 (Ph**C**), 123.9 (Ph**C**), 125.3 (Ph**C**), 129.1 (Ph**C**), 129.5 (Ph**C**), 130.9 (Ph**C**), 131.9 (Ph**C**), 132.0 (Ph**C**), 138.1 (Ph**C**), 138.7 (Ph**C**), 149.5 (Ph**C**), 155.4 (Ph**C** adjunct to N), 157.4 (Ph**C** adjunct to N), 166.9 (**C** in COOMe), 195.2 (**C**=O); FT-IR (KBr, cm^{-1}); 2926(m), 2851(w), 2212(w), 1719(m), 1686(s), 1509(m), 1438(w), 1354(w), 1278(s), 1132(m), 1101(w), 1017(m), 955(m), 831(s), 777(m), 624(s); HRMS (FAB); calcd for $C_{83}H_{66}N_2O_5S_3$, m/z 1266.41; Found: 1266.4098; UV–Vis (in CH_2Cl_2, λ_{max}, nm): 290 nm, 310 nm, 370 nm.

Immobilization of tripod 4 on gold surface

The gold surface was prepared on a mica surface by evaporation in vacuum and kept in the container under vacuum (10^{-6} Pa) before use. The gold substrate was cut to 5 × 7 mm^2 by a ceramic scissor and annealed by heating in a muffle furnace (Isuzu Seisakusho Co. Ltd.) at 400 °C for 3 h, which was subsequently cooled to room temperature under N_2 atmosphere. The gold substrate samples with tripod molecule **4** were prepared under nitrogen atmosphere inside of the glove box and under the following conditions; (*method A*) the annealed gold substrate was immediately soaked in a 2 mL THF (HPLC grade) solution (0.1 µM) of **4** for 3 min, (*method B*) the annealed gold substrate was soaked in a mixture of 2 mL THF solution (0.1 µM) of **4** and 60 µL of aqueous NH_4OH solution for 3 min and subsequently rinsed with THF, (*method C*) same as *method B* and subsequently thoroughly washed with milli-Q water. All the substrates were quickly dried and applied to STM measurements.

STM imaging of a tripod 4 on the gold surface

STM imaging of **4** was carried out in air using Nanoscope E (Digital Instrument, CA, USA) system with V_s = 100–200 mV, I_t = 1–2 nA.

Immobilization of tripod molecular tip A on gold surface

The preparation of molecular tip **A** was carried out *in situ* by the combination of (1) conversion from thioacetate group to thiol and (2) S–Au formation reaction of thiol and the gold substrate. In a solution of **13** in THF (HPLC grade, Aldrich-Sigma, Co. Ltd.) in a vial, NH_4OH (28% NH_3 in water, Aldrich-Sigma, Co. Ltd.) was added and the mixture was incubated for a few minutes in the dark to provide **A**. The clean Au substrate was soaked in this reaction solution for less than 3 min and immediately rinsed with pure THF and milli-Q water. All of the process above was carried out under N_2 atmosphere in a glove box.

Immobilization of tripod molecular tip B on gold surface

To a solution of **14** (4.2 mg, 0.0033 mmol) in THF (5 mL), a solution of NaOH (40 mg, 1 mmol) in methanol (5 mL) was added. The mixture was refluxed in Ar atmosphere for 2 h (TLC monitoring), cooled, and dilute hydrochloric acid (10%, 5 mL) was added. The resulting precipitate was dissolved in CH_2Cl_2. The organic extract was washed with water, brine, dried over anhydrous $MgSO_4$, and concentrated to give **B** as an orange solid. R_f 0.1 (hexane–CH_2Cl_2 (1 : 10)); ^{1}H-NMR (500 MHz, DMSO-d_6) δ 2.13 (brs, 12H, –C**H**$_2$– in adamantane), 3.46 (s, 6H, –C**H**$_2$–SH), 7.2–7.8 (m, 28H, Ar**H**), 7.8–8.0 (m, 8H, Ar**H**); MS (MALDI-TOF) m/z 1127 ([M]$^+$).

Light irradiation

A 100 W Xe lamp with a cold mirror system and band-pass filters LAX-101 (Asahi Spectra, Co. Ltd., Tokyo, Japan) was used as a light source. UV irradiation was carried out with filtering by a mirror module (250–400 nm) and a band pass filter (360 ± 10 nm). Visible light irradiation was carried out with filtering by a mirror module (370–800 nm) and a band pass filter (450 ± 10 nm). The UV and visible light irradiation of the solution was carried out in quartz cells in 0.1 µM solution in CH_2Cl_2 for 10 min 2 cm and 1 cm, respectively, from the fiber and the UV–Vis spectrum of the each solution was measured immediately after using a

double-beam UV–Vis recording spectrophotometer UV-265 (SHIMAZU, Kyoto, Japan). For the irradiation of the AFM tip, the same light source and filters were used and the light from the fiber was focused at the tip using a quartz lens system located outside the UHV chamber for SPM. The amount of photons reaching the sample surface was estimated to be 3×10^2 photons nm^{-2} s^{-1} from the transparency through the quartz and distance to the sample from the fiber.

NC-AFM imaging of molecular tip A immobilized on the gold surface

The prepared gold substrate with molecular tip **A** was dried for several days in the UHV chamber and additional baking (chamber temperature <100 °C) for 7 h. NC-AFM imaging was carried out using JSPM-4610A (JEOL, Tokyo, Japan) in UHV condition at room temperature with $V_s = -0.4$ V, $\Delta f = -72$ Hz, $A_{p\text{-}p} = 12$ nm.

NC-AFM imaging of molecular tip B immobilized on the gold surface

NC-AFM imaging of molecular tip **B** was carried out in UHV (10^{-8} Pa) using JSPM-4610A (JEOL Co. Ltd., Tokyo, Japan) system at room temperature with $V_s = -0.4$ V, $\Delta f = -72$ Hz, and $A_{p\text{-}p} =$ 12 nm. The gold substrate with molecular tip **B** was dried in the UHV condition with chamber baking (chamber temperature <100 °C for 7 h) to remove the water molecules on the surface, which are adsorbed in ambient air after sample preparation and disturb the stable NC-AFM measurement in UHV.

Acknowledgements

The authors thank Dr Naoki Sugimoto and Dr Yuji Haishima in the National Institute of Health Sciences (Japan) for their help in FAB–MS measurements. The authors thank Dr Masaaki Kurihara in the National Institute of Health Sciences (Japan) for fruitful discussion on the synthesis and characterization of the molecules. The authors thank Dr Yasuyuki Yokota in Tokyo Institute of Technology for fruitful discussion of surface analysis. The authors thank Dr Rashid N. Nadaf in Osaka University for partial contribution on the synthesis of molecules. This study was supported in part by Grant-in-Aid for Scientific Research on Advanced Medical Technology (YY) from the Ministry of Labour, Health and Welfare of Japan (Nano-medicine project), Grant-in-Aid for Scientific Research (KF, No. 16310071) and Grant-in-Aid for Young Scientists B (DT, No. 19710090) from the Ministry of Education, Culture, Sports, Science and Technology of Japan, SHISEIDO grants for Scientific Research (KF), JST PRESTO program (YY, KF), and the Nano/Bio Interface Center of University of Pennsylvania through the National Science Foundation (YY, NSEC DMR-0425780).

Notes and references

1 G. Binnig, C. F. Quate and Ch. Gerber, *Phys. Rev. Lett.*, 1986, **56**, 930.
2 C. D. Frisbie, L. F. Rozsnyai, A. Noy, M. S. Wrighton and C. M. Lieber, *Science*, 1994, **265**, 2071.
3 S. S. Wong, E. Joselevich, A. T. Woolley, C. L. Cheung and C. M. Lieber, *Nature*, 1998, **394**, 52.
4 Y. Yao and J. M. Tour, *J. Org. Chem.*, 1999, **64**, 1968.
5 X. Deng and C. Cai, *Tetrahedron Lett.*, 2003, **44**, 815.
6 Q. Li, A. V. Rukavishnikov, P. A. Petukhov, T. O. Zaikova and J. F. W. Keana, *Org. Lett.*, 2002, **4**, 3631.
7 Q. Li, A. V. Rukavishnikov, P. A. Petukhov, T. O. Zaikova, C. Jin and J. F. W. Keana, *J. Org. Chem.*, 2003, **68**, 4862.
8 Q. Li, C. Jin, P. A. Petukhov, A. V. Rukavishnikov, T. O. Zaikova, A. Phadke, D. H. LaMunyon, M. D. Lee and J. F. W. Keana, *J. Org. Chem.*, 2004, **69**, 1010.
9 S. Zarwell and K. Rück-Braun, *Tetrahedron Lett.*, 2008, **49**, 4020.
10 P. Hinterdorfer and Y. F. Dufrene, *Nat. Methods*, 2006, **3**, 347.
11 H. Rau, *Angew. Chem., Int. Ed. Engl.*, 1973, **12**, 224.
12 D. Takamatsu, Y. Yamakoshi and K. Fukui, *J. Phys. Chem. B*, 2006, **110**, 1968.
13 D. T. Gryko, C. Clausen, K. M. Roth, N. Dontha, D. F. Bocian, W. G. Kuhr and J. S. Lindsey, *J. Org. Chem.*, 2000, **65**, 7345.
14 S. Thorand and N. Krause, *J. Org. Chem.*, 1998, **63**, 8551.
15 O. H. Wheeler and D. Gonzalez, *Tetrahedron*, 1964, **20**, 189.
16 S. Sellarajah, T. Lekishvili, C. Bowring, A. R. Thompsett, H. Rudyk, C. R. Birkett, D. R. Brown and I. H. Gilbert, *J. Med. Chem.*, 2004, **47**, 5515.
17 B. Priewisch and K. Rück-Braun, *J. Org. Chem.*, 2005, **70**, 2350.
18 E. F. V. Scriven, H. Suschitzky and G. V. Garner, *Tetrahedron Lett.*, 1973, **14**, 103.
19 Data are provided in the supporting materials†.
20 J. M. Tour, L. Jones II, D. L. Pearson, J. J. S. Lamba, T. P. Burgin, G. M. Whitesides, D. L. Allara, A. N. Parikh and S. V. Atre, *J. Am. Chem. Soc.*, 1995, **117**, 9529.
21 L. Cai, Y. Yao, J. Yang, D. W. Price Jr. and J. M. Tour, *Chem. Mater.*, 2002, **14**, 2905.
22 F.-R. F. Fan, Y. Yao, L. Cai, L. Cheng, J. M. Tour and A. J. Bard, *J. Am. Chem. Soc.*, 2004, **126**, 4035.
23 M. E. Drew, A. Chworos, E. Oroudjev, H. Hansma and Y. Yamakoshi, *Langmuir*, 2010, **26**, 7117.
24 D. Takamatsu, Y. Yamakoshi and K. Fukui, *e-J. Surf. Sci. Nanotechnol.*, 2006, **4**, 249.
25 S. Morita, R. Wiesendanger and E. Meyer, *Noncontact Atomic Force Microscopy*, Springer-Verlag: Berlin, Heidelberg, New York, 2002.
26 A. Sasahara, H. Uetsuka, T. Ishibashi and H. Onishi, *Appl. Surf. Sci.*, 2002, **188**, 265.
27 N. Tamai and H. Miyasaka, *Chem. Rev.*, 2000, **100**, 1875.
28 L. A. Bumm, J. J. Arnold, M. T. Cygan, T. D. Dunbar, T. P. Burgin, L. Jones II, D. L. Allara, J. M. Tour and P. S. Weiss, *Science*, 1996, **271**, 1705.
29 A. Nakasa, U. Akiba and M. Fujihira, *Appl. Surf. Sci.*, 2000, **157**, 326.
30 Y. Yokota, A. Miyazaki, K. Fukui, T. Enoki and M. Hara, *J. Phys. Chem. B*, 2005, **109**, 23779.
31 S. Wakamatsu, S. Fujii, U. Akiba and M. Fujihira, *Nanotechnology*, 2003, **14**, 258.
32 S. Wakamatsu, S. Fujii, U. Akiba and M. Fujihira, *Nanotechnology*, 2004, **15**, S137.
33 M. J. Comstock, N. Levy, A. Kirakosian, J. Cho, F. Lauterwasser, J. H. Harvey, D. A. Strubbe, J. M. J. Fréchet, D. Trauner, S. G. Louie and M. F. Crommie, *Phys. Rev. Lett.*, 2007, **99**, 038301–1.
34 S. J. van der Molen, H. von der Vegte, T. Kudernac, I. Amin, B. L. Feringa and B. J. van Wees, *Nanotechnology*, 2006, **17**, 310.
35 A. S. Kumar, T. Ye, T. Takami, B.-C. Yu, A. K. Flatt, J. M. Tour and P. S. Weiss, *Nano Lett.*, 2008, **8**, 1644.

